

IDENTIFICATION OF NEW NEUTRON-RICH RARE-EARTH NUCLEI PRODUCED IN ^{252}Cf SPONTANEOUS FISSION*

R. C. Greenwood, R. J. Gehrke, J. D. Baker and D. H. Meikrantz

Idaho National Engineering Laboratory, EG&G Idaho, Inc., Idaho Falls, Idaho 83415, USA

Abstract

A program of systematic study of the decay properties of neutron-rich rare-earth nuclei with $30\text{ s} < t_{1/2} < 10\text{ min}$, produced in ^{252}Cf spontaneous fission, is currently underway using the Idaho ESOL (Elemental Separation On Line) Facility. The chemistry system used for the rare earth elemental separations consists of two high-performance chromatography columns connected in series and coupled to the ^{252}Cf fission source via a helium gas-jet transport arrangement. The time delay for separation and initiation of γ -ray counting with this system is typically 2-3 min. Significant results which have been obtained to date with this system include the identification of a number of new neutron-rich rare-earth isotopes including ^{155}Pm ($t_{1/2} = 48 \pm 4\text{ s}$) and ^{163}Gd ($t_{1/2} = 68 \pm 3\text{ s}$), in addition to ^{158}Sm which was identified in an earlier series of experiments.

1. Introduction

A comprehensive program of nuclear structure studies of fission products using both on-line chemical and mass-separation techniques has recently been initiated at the INEL. A unique feature of this program, apart from the use of ESOL (Elemental Separation On Line) and ISOL facilities in combination, is the use of ^{252}Cf as the source of the fission products. As illustrated in Fig. 1, the fission-product yield curve for spontaneous fission of ^{252}Cf has significant differences from those of the more conventional thermal-neutron fission in either ^{235}U or ^{239}Pu . Specifically, one notes in ^{252}Cf the narrower valley region and the significantly higher yields for isotopes with $A \geq 150$. Because of the long-standing interest at this laboratory in the deformed rare-earth region our initial experimental thrust has been to exploit the higher yields of the rare-earth fission-product isotopes available in ^{252}Cf . To accomplish this, we have developed a microprocessor controlled high-performance liquid chromatography (HPLC) system¹⁻³

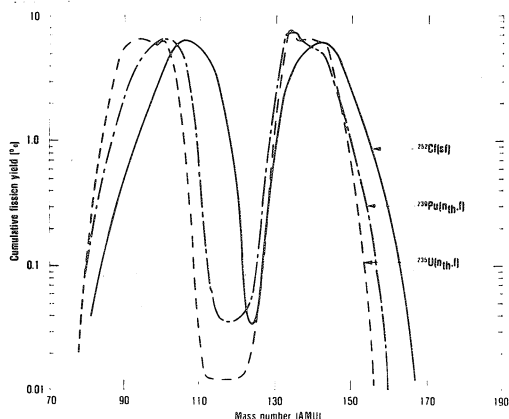


Fig. 1 Comparison of the cumulative yields for spontaneous fission of ^{252}Cf and thermal neutron fission of ^{235}U and ^{239}Pu .

which, at the present stage of development, is capable of providing separated fission-product rare-earth elemental fractions within 2-3 min of the end of sample collection. This HPLC system is coupled on-line to the ^{252}Cf fission sources via a helium gas-jet transport arrangement.⁴)

Because of the relative inaccessibility of this region of more neutron-rich rare-earth isotopes, either from other more conventional fission reactions or from particle-induced reactions, there are many such isotopes with expected half-lives $>30\text{ s}$ which have not previously been observed. As a preliminary step to detailed studies of the structure of nuclides in this region we are presently undertaking a systematic experimental study to observe these unknown isotopes. In this paper we discuss some of the initial results of this effort.

2. The ESOL Facility

2.1 The fission product source

The fission products for this experiment are obtained from two $\sim 300\text{ }\mu\text{g}$ electrodeposits of the spontaneously fissioning isotope, ^{252}Cf .⁵) These sources, which are electrodeposited at Oak Ridge National Laboratory, are located in a specially-designed hot cell,⁶) and are mounted inside a pressurized chamber which forms an integral part of the gas-jet transport arrangement.⁴) A photograph of the source chamber together with one of the ^{252}Cf sources is shown in Fig. 2. The He gas pressure in the chamber is sufficient to thermalize the fission products which then rapidly attach themselves to the NaCl aerosols which have previously been seeded into the He gas stream.⁴) From the source chamber the fission products, now attached to the NaCl aerosols, are transported via a $\sim 25\text{-m}$ capillary (1.3-mm i.d.) to the radiochemistry laboratory. There, they exit into an evacuated chamber, located in the radiochemistry hood, and are collected on mylar tape. After a preset collection time, the mylar tape is moved through a vacuum seal to a wash chamber where the deposited NaCl and



Fig. 2 The ^{252}Cf source chamber and a ^{252}Cf source holder with attached Ni window.

*Work supported by the U. S. Department of Energy under DOE Contract No. DE-AC07-76ID01570.

fission products are washed from the tape with 3M HNO₃. Both the tape movement and wash operations are controlled via a microprocessor. Schematic diagrams of the gas jet transport arrangement and the fission product collection and dissolution system are shown in Figs. 3 and 4, respectively.

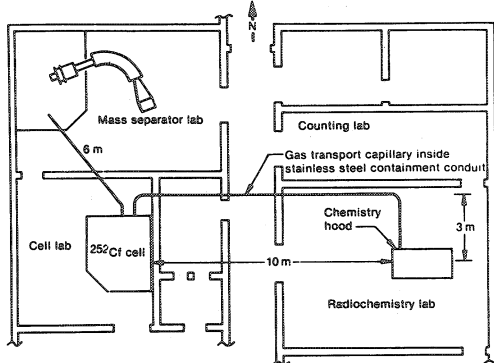


Fig. 3 Schematic floor plan of the laboratories containing the ²⁵²Cf hot cell, the mass separator and the chemistry hood.

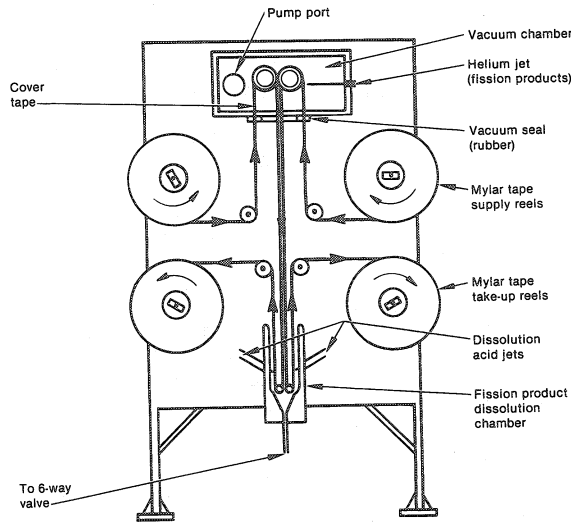


Fig. 4 Automated fission product collection and dissolution apparatus.

2.2 Rare-earth chemistry

The chemical separation of individual rare-earth elemental fractions involves two steps. First, the rare-earth elements are isolated as a group by extraction chromatography. Second, specific separation of the individual rare earths is accomplished by cation exchange. Each of these chemical steps is under the control of a microprocessor. The details of this radiochemical separation technique are given in Refs. 2 and 3. The following is a brief description of the automated radiochemical separation.

After the fission products are washed from the collection tape, they are pumped onto the extraction chromatography column where the rare earths adhere to the extractant, dihexyldiethylcarbonyl-methylene phosphonate (DHDECMP),^{7,8} which is adsorbed on Vydac C₈ resin. After the non rare-earth fission products have passed through the column to waste, the rare earths are eluted with α -hydroxyisobutyric acid (α -HIBA). The eluted rare earths pass to the loop of the injection valve of the second column where they are trapped and subsequently injected onto the cation exchange column which is made

up of Aminex A-9 resin. The rare-earth fission products are eluted in inverse order of Z (i.e., heaviest first) by gradient elution using α -HIBA as the eluent. The individual radio-elements are monitored as they come off the second column with a shielded NaI(Tl) detector. This detector is coupled to a strip chart recorder to provide a chromatogram of the separation. A schematic diagram, together with a photograph, of the high performance liquid chromatography columns coupled in series are shown in Figs. 5 and 6, respectively. Figure 7 shows a chromatogram of a typical separation designed for the separation of the heavier rare-earth fission product fractions, i.e., for Tb and Dy. By changing the program controlling the eluant concentration and pH as a function

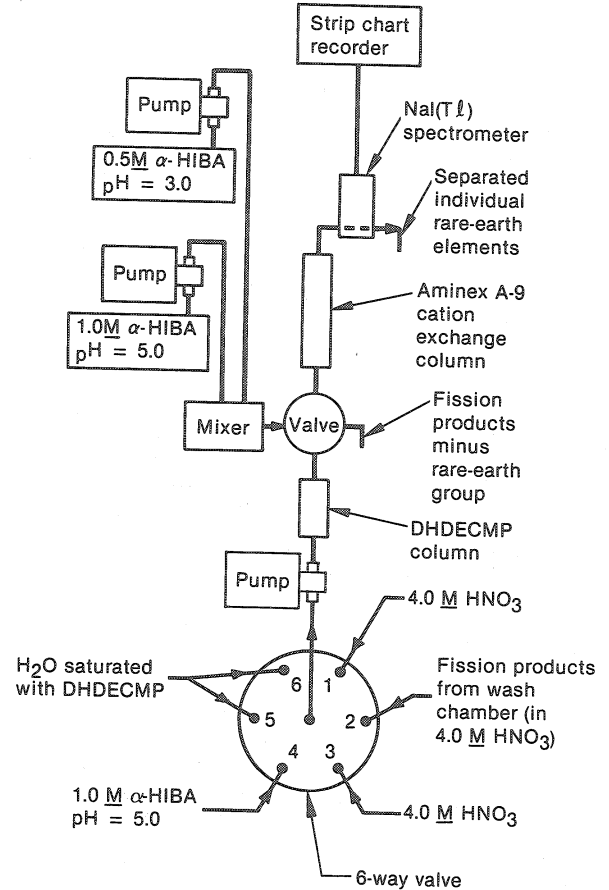


Fig. 5 Schematic diagram of the series coupled HPLC system.

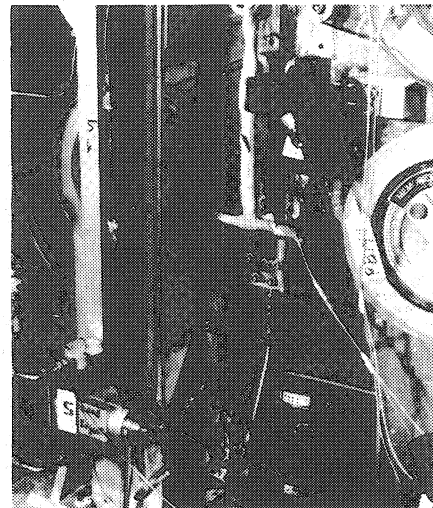


Fig. 6 Photograph showing the two HPLC columns coupled in series.

of time, the higher rare-earth fractions can be separated in shorter times than those shown in Fig. 7.

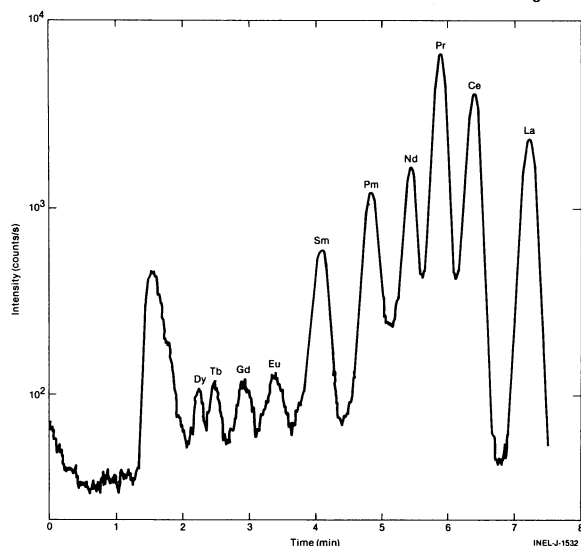


Fig. 7 Typical chromatogram obtained for fission product separations. The time scale is started from the end of the fission product collection period.

2.3 γ -ray measurements

The selected rare-earth elemental fraction, contained in a few drops of solution, is counted at ~ 2 cm source-to-detector distance using a 107-cm^3 coaxial Ge(Li) detector. A 1.235-gm/cm^2 Be absorber is used to reduce the background in the detector associated with the β^- continuum. The resulting 4096 channel pulse height spectra are stored in an Ampex DM 980 80 MByte disc via a PDP 8/E processor. In each experiment a preset sequence of multiscaled 4096 channel γ -ray spectra are obtained following each separation, in order to obtain half-life information for each of the γ -ray lines in the spectra. The availability of the large 80 MByte storage disc allows us to store separately the set of multiscaled spectra obtained following each separation. Following the experiment, the quality of each separation can be assessed and the multiscaled data combined as desired (i.e., data resulting from "bad" separations can be excluded from the final multiscaled spectral sums). For example, in the case of the Pm separation, which is typical of the rare-earth elemental fractions studied, a 2-min He-jet collection was employed and the first γ -ray spectral count was started ~ 3.2 min after the end of the fission-product collection. For each of the 13 radiochemical separations performed, forty 18-s counts were made with a 2-s delay time between each count. Thus, in the completed experiment a total of 520 4096-channel spectra were accumulated.

3. Experimental Measurements and Results

3.1 Measurements

In an earlier series of experiments performed with the series coupled HPLC system, the new isotope, 5.51-min ^{158}Sm , was identified.¹⁾ Since that time the speed of the radiochemical separation has been improved (by greater than a factor of 2) and larger ^{252}Cf sources have been acquired. With these improvements in the ESOL facility, it therefore seemed profitable to renew our search for new neutron-rich rare-earth isotopes. In this most recent series of experiments, elemental fission-product fractions

of Nd, Pm, Sm, Eu, Gd, Tb and Dy were separated and individually γ -ray counted in the multiscaled mode. Analysis of these data is presently being carried out. The results reported in this present paper are from analysis of the data from the Pm and Gd fractions.

3.2 The ^{155}Pm isotope

In Fig. 8 we show the lower energy portions of the first and fifth (i.e., 80-s time separation between them) multiscaled spectra summed over the 13 Pm separations performed. The activities observed in this spectrum are 4.1-min ^{152}Pm , 7.5-min ^{152}Pm , 5.4-min ^{153}Pm , 1.7-min ^{154}Pm , 2.7-min ^{154}Pm , 46.8-h ^{153}Sm (later spectra only), 22.4-min ^{155}Sm , 12.4-min ^{151}Nd , 11.4-min ^{152}Nd and a 48-s activity identified in this study as ^{155}Pm . The 725- and 778-keV γ rays in Fig. 8 are the most prominent which can be associated with this latter activity. As seen from the figure, they are clearly decaying at a much faster rate than those γ rays which can uniquely be associated with the decay of the 1.7-min ^{154}Pm (e.g., the 839-keV peak).

The assignment of the 48-s activity to ^{155}Pm is based on the following three observations:

1. the activity is present only in the Pm fraction, it is not observed in either of the adjacent Nd or Sm fractions;
2. the intensity of the 104-keV γ ray emitted in the decay of 22.4-min ^{155}Sm increased throughout the first 7 multiscaled spectra, indicating that it is being fed by a ~ 50 -s parent activity (as illustrated in Fig. 9); and
3. the prominent 725- and 778-keV γ rays can be placed in a consistent fashion into the level scheme of ^{155}Sm proposed by Smither et al.⁹⁾ from studies of the $^{154}\text{Sm}(n,\gamma)$ reaction.

A summary of the γ -ray energies and relative intensities which can be associated with the ^{155}Pm decay is given in Table 1. A value of 48 ± 4 s was obtained for the half-life of this isotope, based on the decay rates of the 409-, 725- and 778-keV γ rays. From a comparison of the relative intensities of the 104-keV γ ray in the ^{155}Sm daughter (using a value of 70 ± 6 γ rays per 100 decays for its intensity¹⁰⁾) to that of the 778-keV γ ray in the ^{155}Pm parent we obtain a value of 7.9 ± 0.8 γ rays per 100 decays for the absolute intensity of the 778-keV γ ray. (In obtaining this value, a correction was made to the 104-keV γ -ray intensity for the ^{155}Sm initially present as a contaminant in the Pm fraction following the separation.)

From the level assignments for ^{155}Sm of Smither et al.,⁹⁾ the γ rays shown in Table 1 are quite straightforwardly fit into a decay scheme for ^{155}Pm as illustrated in Fig. 10. The prominent decay into the spin-3/2 member of the $3/2^- [532]$ band in ^{155}Sm is analogous to that in the decay of ^{153}Pm . In fact, if we assume a Q value of 3.1 MeV for the decay of ^{155}Pm ,¹¹⁾ this branching rate yields a log ft value of 5.6, which is essentially identical to the value of 5.5 reported¹⁰⁾ for the same transition in ^{153}Pm decay. Such a fast transition is, as has been proposed for ^{155}Pm , consistent with $5/2^- \rightarrow 5/2^- [532]$ assignment to the ^{155}Pm ground state.

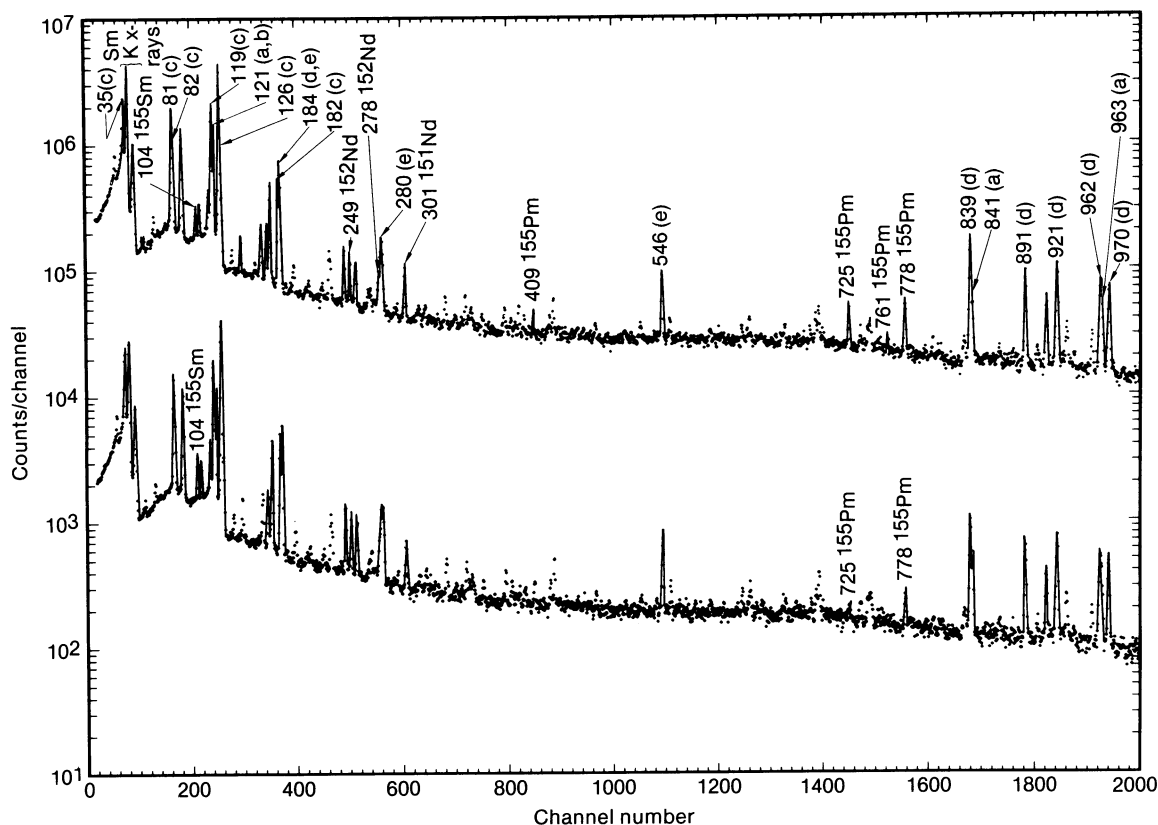


Fig. 8 Lower energy portion of the first (upper) and fifth (lower) multiscaled γ -ray spectra, with a time separation of 80 s, measured with the Pm fraction. The γ -ray peaks are identified by the following key: (a) 4.1-min ^{152}Pm ; (b) 7.5-min ^{152}Pm ; (c) 5.4-min ^{153}Pm ; (d) 1.7-min ^{154}Pm ; and, (e) 2.7-min ^{154}Pm

Table 1. Energies and relative intensities of the γ rays associated with the decay of ^{155}Pm

γ -ray energy (keV)	Relative γ -ray intensity
53.1(5)	12(2)
409.8(2)	28(2)
725.4(2)	68(3)
762.0(3)	19(4)
778.6(2)	100

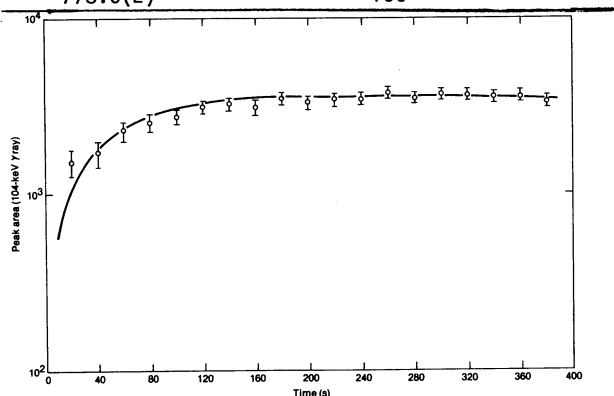


Fig. 9 Grow-in of the 104-keV γ ray from the 22.4-min ^{155}Sm decay as a function of time after separation.

3.3 The ^{163}Gd isotope

In Figs. 11 and 12 we show the first and fourth (i.e., 3-min separation time between them) multiscaled spectra of the Gd fraction, summed over all

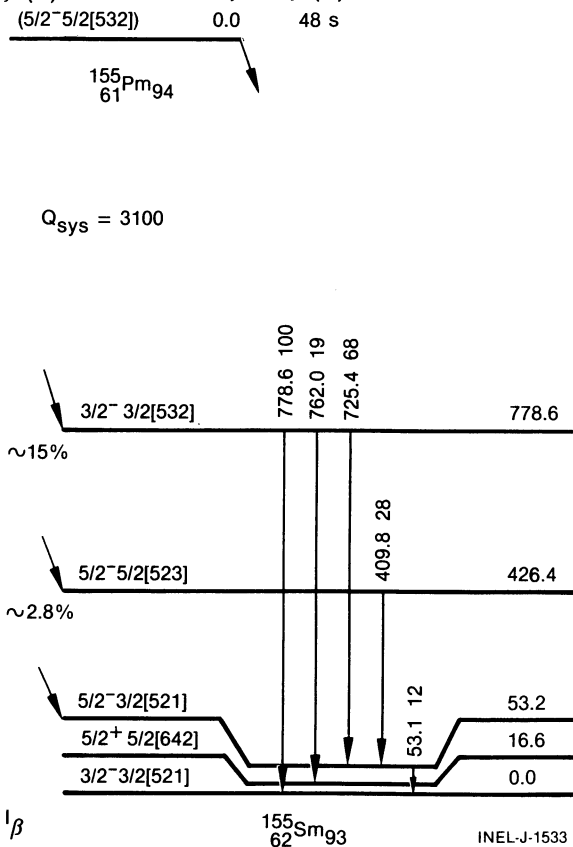


Fig. 10 Proposed decay scheme for the 48-s ^{155}Pm isotope.

of the individual Gd separations. The activities observed in this spectrum are 3,6-min ^{161}Gd , 9-min ^{162}Gd , 7,7-min ^{162}Tb , 19-min ^{163}Tb , Sm and Eu contaminants and a 68-s activity identified in this study to be ^{163}Gd .

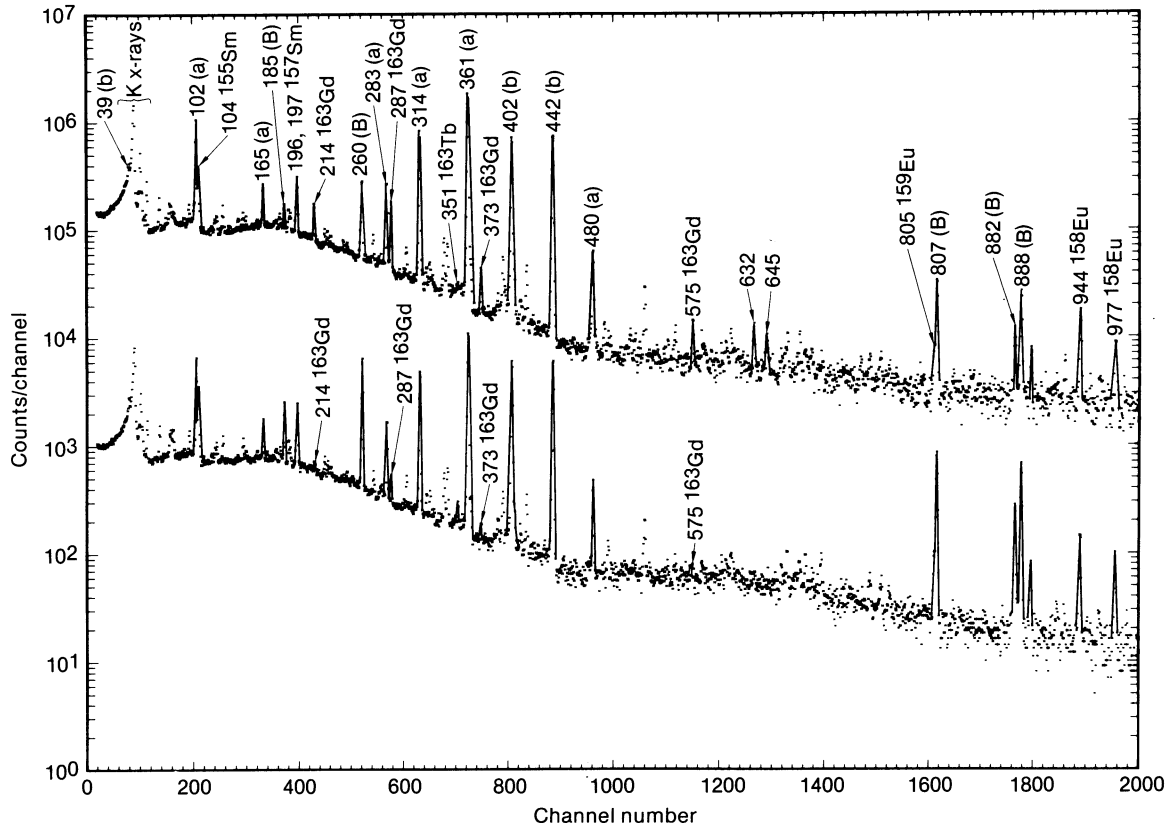


Fig. 11 The first (upper) and fourth (lower) multiscaled γ -ray spectra, with a time separation of 3.0 min, measured with the Gd fraction. The γ -ray peaks are identified by the following key: (a) ^{161}Gd , (b) ^{162}Gd ; and, (B) ^{162}Tb .

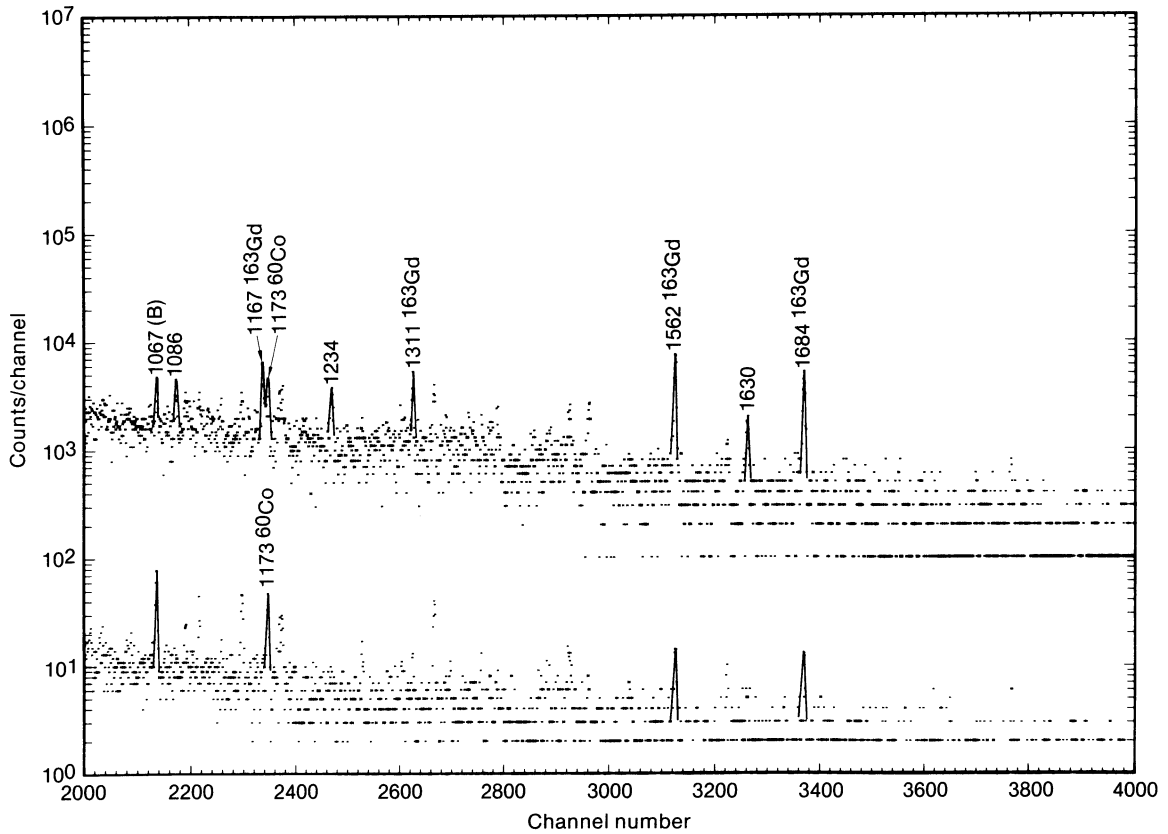


Fig. 12 The first (upper) and fourth (lower) multiscaled γ -ray spectra, with a time separation of 3.0 min, measured with the Gd fraction. The γ -ray peaks are identified by the following key: (a) ^{161}Gd , (b) ^{162}Gd ; and, (B) ^{162}Tb .

The assignment of the 68-s activity to ^{163}Gd is based on the following: (1) the γ -ray lines associated with this activity are present only in the Gd fraction; and (2) the grow-in of the 351-keV γ ray emitted by 19-min ^{163}Tb is consistent with its being fed by a 68-s parent activity (as illustrated in Fig. 13).

A summary of the energies and relative intensities of the γ rays which can be associated with the ^{163}Gd decay is given in Table 2. A value of 68 ± 3 s was obtained for the half-life of ^{163}Gd based on an average of each of the decay rates of the γ -rays shown in Table 2. A value of 16 ± 3 γ rays per 100 decays was obtained for the absolute intensity of the 287-keV γ ray based upon comparison of its intensity with that of the 351-keV γ -ray emitted in the decay of 19-min ^{163}Tb (with an absolute intensity of 26.3 ± 0.4 γ rays per 100 decays¹⁰).

Table 2. Energies and relative intensities of the γ rays associated with the decay of ^{163}Gd

γ -ray energy (keV)	Relative γ -ray intensity
214.0(3)	46(3)
287.8(3)	100
373.4(3)	25(2)
575.1(3)	11(2)
1167.8(3)	20(2)
1311.6(3)	13(5)
1562.0(3)	36(3)
1684.5(3)	32(3)

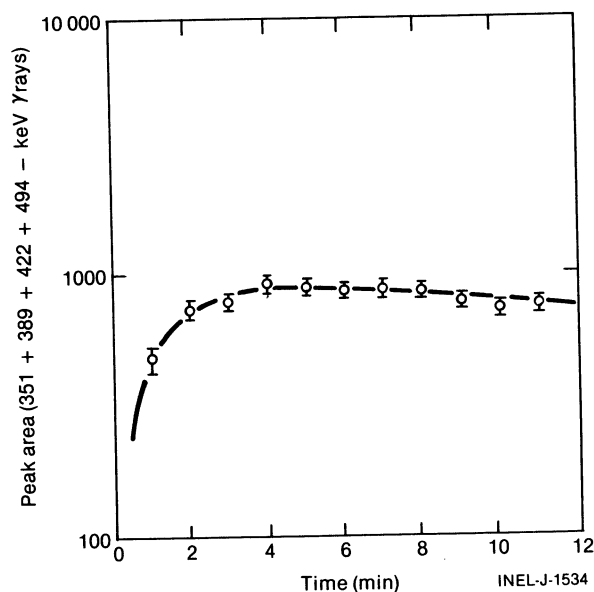


Fig. 13 Grow-in of the γ rays from the 19.5-min ^{163}Tb decay as a function of time after separation.

4. References

1. J. D. Baker, R. J. Gehrke, R. C. Greenwood, D. H. Meikrantz and V. J. Novick, *J. Inorg. Nucl. Chem.* **42** (1980) 1547.
2. J. D. Baker, R. J. Gehrke, R. C. Greenwood and D. H. Meikrantz, *Radiochim. Acta* **28** (1981) 51.
3. J. D. Baker, R. J. Gehrke, R. C. Greenwood and D. H. Meikrantz, to be published.
4. R. C. Greenwood, R. A. Anderl, R. J. Gehrke and S. T. Croney, U. S. ERDA Report TREE-1116 (1977) p. 76.
5. ^{252}Cf sources made available through J. E. Bigelow, Coordinator for the National Transplutonium Element Production Program, Oak Ridge National Laboratory, Oak Ridge, TN 37830, USA.
6. R. A. Anderl and C. H. Cargo, *Proc. 27th Conf. Remote Systems Technology* (1979) p. 347.
7. L. D. McIsaac, J. D. Baker and J. W. Tkachyk, U. S. ERDA Report ICP-1080 (1975).
8. L. D. McIsaac, J. D. Baker, J. F. Krupa, R. E. LaPointe, D. H. Meikrantz and N. C. Schroeder, U. S. DOE Report ICP-1180 (1979).
9. R. K. Smither, K. Schreckenbach, H. G. Börner, W. F. Davidson, T. von Egidy, D. D. Warner, R. F. Casten, M. L. Stelts and A. I. Namenson, Argonne National Laboratory Report ANL-80-94 (1980) p. 90; and, R. K. Smither, private communication.
10. C. M. Lederer and V. S. Shirley (Editors), *Table of Isotopes*, 7th ed. (Wiley, New York, 1978).
11. A. H. Wapstra and K. Bos, *At. Data Nucl. Data Tables* **19** (1977) 215.